DOE/ER/05002-25

SECONDARY GRAIN-BOUNDARY DISLOCATIONS IN [001] TWIST BOUNDARIES IN MgO. II. EXTRINSIC STRUCTURES

C. P. Sun† and R. W. Balluffi

Department of Materials Science and Engineering
Massachusetts Institute of Technology
Cambridge, Massachusetts 02139

DOE/ER/05002--25

DE82 011169

December 1981

Massachusetts Institute of Technology
Cambridge, Massachusetts 02139

Prepared for

U.S. Department of Energy
under Contract DE-AS02-78ER05002

---

† Now at Thomas J. Watson Research Center, IBM Corp., Yorktown Heights, New York 10598.

DISCLAIMER

ABSTRACT

Extrinsic secondary grain boundary dislocation (GBD) structures were observed by weak beam transmission electron microscopy in a variety of [001] twist boundaries in MgO. These structures were derived from segments of lattice dislocations embedded in the boundaries and could be interpreted as the result of the decomposition of the lattice dislocations into extrinsic GBDs and the subsequent interaction of the product GBDs with the intrinsic boundary structure. The results demonstrate that lattice dislocations in MgO are attracted to grain boundaries over a wide range of conditions and tend to remain embedded in the boundaries as extrinsic GBD structures. All observations could be rationalized on the basis of the CSL model for grain boundaries in cubic materials and were consistent with the intrinsic boundary structures described in Part I of the present work (Sun and Balluffi 1981). Furthermore, the results were similar in many respects to earlier results obtained with [001] twist boundaries in gold.

1. INTRODUCTION

In Part I of the present work (Sun and Balluffi 1981) we described intrinsic secondary grain boundary dislocation (GBS) structures observed by transmission electron microscopy in [001] twist boundaries in MgO. These consisted of uniform arrays of screw and edge GBDs which accommodated twist deviations from low Σ† misorientations and relatively small tilt components respectively. The results were found to be entirely consistent with the CSL† model for grain boundaries in cubic materials.

In the present paper (Part II of our work) we describe closely related observations of extrinsic GBD structures in these same boundaries. Extrinsic GBDs are defined as extra GBDs which are present in the boundary in a more or less disorganized fashion and which do not act in a systematic way to accommodate the crystal misorientation associated with the boundary as a whole. In the present work these extrinsic GBDs were derived from segments of lattice dislocations embedded in the grain boundaries, and their study provides further insight into the structure of the boundaries and their line defects.

Extrinsic GBD structure of this type has been investigated previously in twist and tilt boundaries in gold (Schober and Balluffi 1971; Darby, Schindler and Balluffi 1978). Additional work on interactions between lattice dislocations and grain boundaries has been carried out by Pond and Smith (1977). Preliminary reports of some of the present work in its early stages have been published elsewhere (Sun and Balluffi 1979; Balluffi, Bristowe and Sun 1981).

---

† $\Sigma \equiv$ reciprocal of fraction of lattice atoms in coincidence; CSL $\equiv$ Coincidence Site Lattice.

2. EXPERIMENTAL

The bicrystal specimens were prepared by welding two single crystals together under pressure according to the technique described briefly in Part I (Sun and Balluffi 1981) and in more detail by Sun (1980). Thin film specimens containing sections of grain boundary suitable for transmission electron microscopy were then obtained by a series of mechanical cutting, mechanical polishing and electropolishing operations. Extrinsic GBD structures were observed in essentially all of the boundaries observed which were derived from segments of lattice dislocations embedded in the intrinsic boundary structure. The presence of these structures could have been due to either: (1) lattice dislocations which were generated in the bicrystal after the initial welding contact and then impinged on the grain boundary, or (2) lattice dislocation segments which were required topologically in the grain boundary because of the prior existence of lattice dislocations in the two crystals making up the bicrystal which intersected the two free surfaces which were welded together. In any case, each welded specimen was vacuum annealed at 1500°C for 1 h just before the final thinning by electropolishing, and this treatment tended to equilibrate locally the extrinsic GBD structures which were observed.

Further details of the experimental procedures are described in Part I (Sun and Balluffi 1981).

3. INTERACTION OF LATTICE DISLOCATIONS WITH GRAIN BOUNDARIES

As pointed out above, all of the observed extrinsic GBD structures were derived from segments of lattice dislocations embedded in the grain boundaries.

For purposes of analysis it is therefore convenient to consider the final observed structures to be the result of the following hypothetical three-stage process, even though it is realized that the actual extrinsic GBD structure may not have formed in just this way:

(i) placement of a segment of lattice dislocation in the intrinsic boundary;

(ii) decomposition of the lattice dislocation into extrinsic GBDs;

(iii) interaction of the product GBDs with the intrinsic boundary structure.

The decomposition in Step (ii) can be analyzed effectively within the framework of the CSL model (see Part I) for grain boundaries. According to this model it is always geometrically possible for a lattice dislocation to dissociate into an integral number of perfect GBDs while conserving the total Burgers vector (Pond and Smith 1977; Darby, Schindler and Balluffi 1978). This comes about since the Burgers vectors of all lattice dislocations and perfect GBDs are vectors of the same DSC-Lattice. Thus, the conservation of Burgers vector strength can be written as

$$\underline{b}_L = \sum_i n_i \underline{b}_i \qquad (1)$$

for the dissociation of a lattice dislocation into i different types of GBDs. Here, n_i is the integral number of i type GBDs formed, and $\underline{b}_L$ and $\underline{b}_i$ are the Burgers vectors of the lattice dislocation and product GBDs respectively. Since $|\underline{b}_L|$ is generally larger than $|\underline{b}_i|$, the decomposition usually proceeds with a decrease of elastic energy which then acts as a driving force for the reaction.

4. RESULTS

4.1 Σ = 1, 5, 17, 25, 29 and 53 Boundaries

Segments of extrinsic GBD structures were found in boundaries close to the exact Σ = 1, 5, 17, 25, 29 and 53 misorientations which could be interpreted on the basis of the decomposition of lattice dislocations of the type a/2<110> into integral numbers of distinguishable GBDs of type $\underline{b}_1$, $\underline{b}_2$ and $\underline{b}_3$ and their subsequent interactions with the boundary. A "$\underline{b}_3$ type" vector is defined as any vector of the DSC-Lattice family $\underline{b}_3$, $\underline{b}_4$, $\underline{b}_5$ and $\underline{b}_6$, all of which possess a component perpendicular to the boundary plane given by a/2[001]. These vectors are illustrated in Fig. 2 of Part I and listed in Table 1 of Part I (Sun and Balluffi 1981). Since a variety of lattice dislocations possessing Burgers vectors of the type a/2<110> exist in the MgO structure a variety of possible decompositions into GBDs existed which, in turn, led to a variety of final extrinsic GBD configurations in the boundary. A tabulation of the possible decompositions of lattice dislocations, consistent with the relation

$$\underline{b}_L = n_1 \underline{b}_1 + n_2 \underline{b}_2 + n_3 \underline{b}_3 \quad , \tag{2}$$

is given in Table 1. For lattice dislocations with Burgers vectors parallel to the boundary, i.e., $\underline{b}_L$ = (a/2)[±1 ±1 0], n_3 = 0, there is only one type of $(n_1,n_2,0)$ combination for dissociation in each CSL boundary. These are designated as Type (i) dissociations. For lattice dislocations with Burgers vectors inclined to the boundary, i.e., $\underline{b}_L$ = (a/2)[±1 0 ±1] or (a/2)[0 ±1 ±1], the dissociation products must include a $\underline{b}_3$ type GBD (n_3 = ±1). There are four possible dissociations of this type in each CSL boundary. These are designated as Type (ii)-(v) dissociations. Also listed in Table 1 are the changes in elastic energy due to the dissociations

calculated approximately by the usual method of taking the energy of each dislocation to be proportional to the square of its Burgers vector. Appreciable energy reductions occur in most cases, as expected. However, several energy changes are zero and one, i.e., the $\Sigma = 5$ Type (v) dissociation, is actually positive. Since $\underline{b}_1$ and $\underline{b}_2$ tend to decrease in magnitude as Σ increases the reduction in energy generally tends to increase as Σ increases. Also, the energy reduction tends to be smaller for dissociations involving a $\underline{b}_3$ GBD, since $\underline{b}_3$ is relatively large.

An asterisk is placed next to each dissociation in Table 1 which was observed experimentally, and it is seen that a majority of the possible dissociations was observed including cases where the estimated change in elastic energy was either zero or positive [i.e., the $\Sigma = 5$ Type (v) case]. In considering these latter results in particular it must be emphasized that the total energy change includes additional terms which may cause it to become negative in certain cases and therefore favorable. These include changes in the total dislocation core energy and the interaction energy with the intrinsic structure of the boundary.

As shown in Part I (Sun and Balluffi 1981), the intrinsic structure of the $\Sigma = 1$, 5, 17, 25, 29 and 53 boundaries contained square grids of $\underline{b}_1$ and $\underline{b}_2$ screw GBDs. When a lattice dislocation dissociated in the boundary any $\underline{b}_1$ and $\underline{b}_2$ product GBDs therefore took their place as extra GBDs squeezed into the otherwise perfect grid. On the other hand, any $\underline{b}_3$ type GBDs interacted with the intrinsic screw GBD network grid to form line defects of the $\underline{b}_e^{eff}$ type GBDs already described in Section 3.2 of Part I (Sun and Balluffi 1981) and illustrated schematically in Fig. 6 of Part I. In this interaction the $\underline{b}_3$ type GBD broke up into segments which in turn interacted with

the intrinsic screw GBDs causing them to become displaced across the line defect by a distance corresponding to half their spacing in the network. Detailed discussions of these reactions have been given previously by Schober and Balluffi (1971), Balluffi, Komem and Schober (1972) and Sun (1980). In the following we describe a few typical examples.

$\Sigma = 1$: Fig. 1 shows extrinsic GBD structures produced by the reaction of lattice dislocations with a ($\Sigma = 1$, $\theta = 2.5°$) boundary. Examples include Type (i) and (ii) reactions where the lattice dislocation was of the $\underline{b}_1$, $\underline{b}_2$ or $\underline{b}_3$ type. See the figure caption for more details.

$\Sigma = 29$: Fig. 2 shows an extrinsic GBD structure in a $\Sigma = 29$, $\theta = 43.6°$ boundary which decomposed by a Type (i) reaction into two $\underline{b}_1$ and five $\underline{b}_2$ type GBDs which remained squeezed into the screw GBD network as extra screw GBDs. See the figure caption for more details.

$\Sigma = 53$: Fig. 3 shows two extrinsic GBD structures in a boundary near the exact $\Sigma = 53$ misorientation. In each case the lattice dislocation decomposed by a Type (iii) dissociation to produce seven $\underline{b}_1$ or $\underline{b}_2$ GBDs and a single $\underline{b}_3$ type GBD. The $\underline{b}_1$ and $\underline{b}_2$ GBDs remained as extrinsic screw GBDs squeezed into the intrinsic screw GBD network, whereas the $\underline{b}_3$ GBDs interacted with the intrinsic network to form $\underline{b}_e^{eff}$ type GBDs which are characterized by broad diffraction contrast when $\underline{g}$ is almost perpendicular to $\underline{u}$, as in (b), and a lack of contrast when $\underline{g} \parallel \underline{u}$, as in (a); ($\underline{u}$ = GBD tangent vector). See the figure caption for more details.

4.2 $\Sigma = 13$ Boundaries

As shown in Part I (Sun and Balluffi 1981), the intrinsic GBD structure of boundaries near the exact $\Sigma = 13$ misorientation consisted of

a square grid of partial screw GBDs with Burgers vectors given by $\underline{b}_1' = 1/2[\underline{b}_1 + \underline{b}_2]$ and $\underline{b}_2' = 1/2[\underline{b}_1 - \underline{b}_2]$. The background boundary structure consisted of a square checkerboard pattern composed of square patches of the $\Sigma = 13$ boundary possessing different structures to accommodate the partial GBD character of the network (see Fig. 5 of Part I). Figure 4(a) shows an extrinsic structure produced by the dissociation of a lattice dislocation in such a boundary. In this case the lattice dislocation dissociated into six extrinsic partial GBDs according to the reaction

$$\underline{b}_L = 2\underline{b}_1' + 3\underline{b}_2' + \underline{b}_3' = a/2[101] \quad , \tag{3}$$

where $\underline{b}_1' = a/26[230]$, $\underline{b}_2' = a/26[3\bar{2}0]$ and $\underline{b}_3' = a/2[001]$. It is readily shown that the introduction of any of the product partial GBDs produces a change in the boundary structure across the dislocation which corresponds to the difference in structure between the square patches of the intrinsic structure. Therefore, no patches of new boundary structure were produced anywhere by the introduction of these defects. The geometry of the dissociation is shown schematically in Fig. 4(b), and a schematic diagram of the way in which the checkerboard pattern was perturbed is shown in Fig. 4(c). It is interesting to note that no offset of the screw GBDs of the intrinsic network occurs across the $\underline{b}_3'$ GBD in this case. It is seen that a completely self-consistent extrinsic structure may be obtained in this way. This result, therefore, provides additional support for the interpretation of the structure of the $\Sigma = 13$ boundaries in terms of partial GBDs advanced in Part I.

4.3 High Σ Boundaries

In Part I (Sun and Balluffi 1981) it was found that no intrinsic

GBD networks, made up of $\underline{b}_1$ and $\underline{b}_2$ type screw GBDs, could be detected in the angular regimes corresponding to high Σ values which existed between the special low Σ misorientations. On the other hand, easily observable intrinsic $\underline{b}_e^{eff}$ type edge GBDs were always found when tilt components were present. It was concluded that this result was most likely due to the fine spacing and/or weak Burgers vectors of the $\underline{b}_1$ and $\underline{b}_2$ screw GBDs. (We note that the $\underline{b}_e^{eff}$ edge GBDs possess a considerably larger Burgers vector and were generally well spaced out.)

All observations of extrinsic GBD structures produced by the reaction of lattice dislocations with high Σ boundaries in the present work were consistent with these results. In general, any $\underline{b}_1$ or $\underline{b}_2$ GBD produced by the dissociation of a lattice dislocation could not be detected whereas any $\underline{b}_e^{eff}$ type GBD was readily observed. Results for Type (i) and Type (ii) dissociations are shown in Fig. 5 at F and E respectively. In the Type (i) dissociation the Burgers vector of the lattice dislocation is parallel to the boundary and, therefore, only $\underline{b}_1$ and $\underline{b}_2$ GBDs can be produced. As seen at F, these GBDs are not detected, and no extrinsic GBD structure associated with the impingement of the lattice dislocation is visible. On the other hand, in the Type (ii) dissociation the Burgers vector of the lattice dislocation is inclined to the boundary, and a $\underline{b}_3$ GBD is produced by the dissociation. This GBD is easily seen at E in the form of a $\underline{b}_e^{eff}$ GBD after interaction with the boundary. Again, however, no $\underline{b}_1$ or $\underline{b}_2$ GBDs are visible.

5. CONCLUDING REMARKS

The present results demonstrate that lattice dislocations in MgO are attracted to grain boundaries over a wide range of conditions and tend

to remain embedded in the boundaries as extrinsic GBD structures. This appeared to be the case even when the change in elastic energy accompanying dissociation into GBDs in the boundary (calculated on the basis of the squares of the Burgers vectors) was either zero or negative. Evidently, in such cases the change in core energy and the interaction with the intrinsic boundary structure caused the total energy change to go negative. So far, no detailed calculations of this formidable problem have been carried out in support of this result.

All of the extrinsic GBD structures observed could be rationalized on the basis of the CSL model and were consistent with the intrinsic boundary structures found in Part I (Sun and Balluffi 1981). The results, therefore, provide additional support for the CSL model for boundaries in MgO. Furthermore, the results were similar in many respects to the results obtained earlier in studies of intrinsic (Schober and Balluffi 1970) and extrinsic (Schober and Balluffi 1971) GBD structures in [001] twist boundaries in gold.

A major problem in the present work was our inability to detect fine screw GBD structure at high Σ misorientations in angular regimes between a number of the relatively low Σ misorientations studied. In Part I we concluded that such structure is most likely present but is difficult to detect. It would be of considerable interest to demonstrate this conclusively by means of further observations using more powerful techniques.

ACKNOWLEDGMENT

This work was supported by the U.S. Department of Energy under Contract no. DE-AS02 78ER05002.

Table 1. Dissociation reactions, according to Eq. (2), of lattice dislocations into perfect GBDs in CSL boundaries.

Σ	$b_1^2, b_2^2 (a^2)$	$b_3^2 (a^2)$		(n_1, n_2, n_3)	$\Sigma n_i b_i^2 (a^2)$	% Energy Change
1	1/2	1/2	(i)	(1,0,0)*	1/2	0
			(ii)	(0,0,1)*	1/2	0
5	1/10	3/10	(i)	(2,1,0)*	3/10	-40
			(ii)	(1,0,1)*	4/10	-20
			(iii)	(1,1,1)*	5/10	0
			(iv)	(2,0,1)*	5/10	0
			(v)	(2,1,1)*	6/10	20
17	1/34	9/34	(i)	(4,1,0)	5/34	-70
			(ii)	(2,1,1)	12/34	-29
			(iii)	(2,2,1)*	13/34	-24
			(iv)	(3,1,1)	13/34	-24
			(v)	(3,2,1)	14/34	-18
25	1/50	13/50	(i)	(4,3,0)*	7/50	-72
			(ii)	(3,0,1)*	16/50	-36
			(iii)	(3,1,1)*	17/50	-32
			(iv)	(4,0,1)*	17/50	-32
			(v)	(4,1,1)*	18/50	-28
29	1/58	15/58	(i)	(5,2,0)*	7/58	-76
			(ii)	(3,1,1)*	19/58	-34
			(iii)	(3,2,1)*	20/58	-31
			(iv)	(4,1,1)	20/58	-31
			(v)	(4,2,1)	21/58	-28
53	1/106	27/106	(i)	(7,2,0)	9/106	-83
			(ii)	(4,2,1)	33/106	-38
			(iii)	(4,3,1)*	34/106	-36
			(iv)	(5,2,1)	34/106	-36
			(v)	(5,3,1)	35/106	-34
∞	~ 0	$\sim 1/4$	(i)	$(n_1, n_2, 0)$*	~ 0	~ -100
			(ii)	$(n_1, n_2, 1)$*	$\sim 1/4$	~ -50

* Dissociation reaction observed experimentally.

REFERENCES

BALLUFFI, R.W., BRISTOWE, P.D. and SUN, C.P., 1981, J. Amer. Ceram. Soc., 64, 23.

BALLUFFI, R.W., KOMEM, Y. and SCHOBER, T., 1972, Surf. Sci. 31, 68.

DARBY, T.P., SCHINDLER, R. and BALLUFFI, R.W., 1978, Phil. Mag. A, 37, 245.

POND, R.C. and SMITH, D.A., 1977, Phil. Mag., 36, 353.

SCHOBER, T. and BALLUFFI, R.W., 1970, Phil. Mag. 21, 109.

SCHOBER, T. and BALLUFFI, R.W., 1971, Phil. Mag. 24, 165.

SUN, C.P. and BALLUFFI, R.W., 1979, Scripta Met., 13, 757.

SUN, C.P., 1980, Ph.D. Thesis, Cornell University.

SUN, C.P. and BALLUFFI, R.W., 1981, U.S. Department of Energy, Division of Materials Science, Report DOE/ER/05002-24.

FIGURE CAPTIONS

Fig. 1 Extrinsic GBD structures in [001] twist boundary ($\Sigma = 1$, $\theta = 2.5°$). Intrinsic background structure consists of square grid of primary (lattice) screw GBDs. (a) Bright field multi-beam image. Lattice dislocations enter at A, B's and C's. (b) C's indicate entrance points of lattice dislocations possessing $\underline{b}_3$ type Burgers vectors. Curved lines indicate $\underline{b}_e^{eff}$ type GBD structures produced by interaction of these $\underline{b}_3$ type GBDs with intrinsic boundary structure. Resulting offset of screw GBD network across these line defects seen clearly along segments PQ and RS in (a). (c) A and B indicate entrance points of lattice dislocations possessing $\underline{b}_1$ and $\underline{b}_2$ type Burgers vectors respectively. Interaction of these dislocations with intrinsic structure produces extra $\underline{b}_1$ and $\underline{b}_2$ type screw GBDs squeezed into grid.

Fig. 2 Extrinsic GBD structure in [001] twist boundary ($\Sigma = 29$, $\theta = 43.6°$). (a) and (b) Weak beam dark field images formed with 200 and 020 reflections respectively. Intrinsic background structure consists of grid of screw GBDs along <730> . Lattice dislocation enters at arrow and undergoes Type (i) dissociation in boundary. (c) Schematic representation of extrinsic GBD structure.

Fig. 3 Extrinsic GBD structures in [001] twist boundary near exact $\Sigma = 53$ misorientation. (a) and (b) Weak beam dark field images formed with 200 and 020 reflections respectively. Intrinsic background structure consists of grid of screw GBDs along <950> and array of approximately parallel $\underline{b}_e^{eff}$ edge GBDs. Latter GBDs are strong horizontal lines which are out of contrast in (a) where

they are parallel to $\underline{g}$. Lattice dislocations enter at A and B. Each undergoes a Type (iii) dissociation in boundary.

(c) Schematic representation of extrinsic GBD structures.

Fig. 4 Extrinsic GBD structure in [001] twist boundary near exact $\Sigma = 13$ misorientation. (a) Weak beam dark field image formed with 200 reflection. Intrinsic background structure consists of grid of partial screw GBDs along <320> . Lattice dislocation enters boundary at A. (b) Schematic representation of extrinsic partial GBD structure. (c) Schematic representation of perturbed "checkerboard" boundary pattern in vicinity of the extrinsic GBD structure (see text).

Fig. 5 Extrinsic GBD structures in high Σ [001] twist boundaries. Only $\underline{b}_e^{eff}$ type edge GBDs are visible in the background structure. Lattice dislocations enter boundaries at F and E. (a) $\theta = 32.1°$. Burgers vector of lattice dislocation is parallel to boundary and any $\underline{b}_1$ and $\underline{b}_2$ GBDs due to dissociation not visible.

(b) Burgers vector of lattice dislocation inclined to boundary. The $\underline{b}_3$ GBD produced by dissociation is visible as a $\underline{b}_e^{eff}$ GBD.

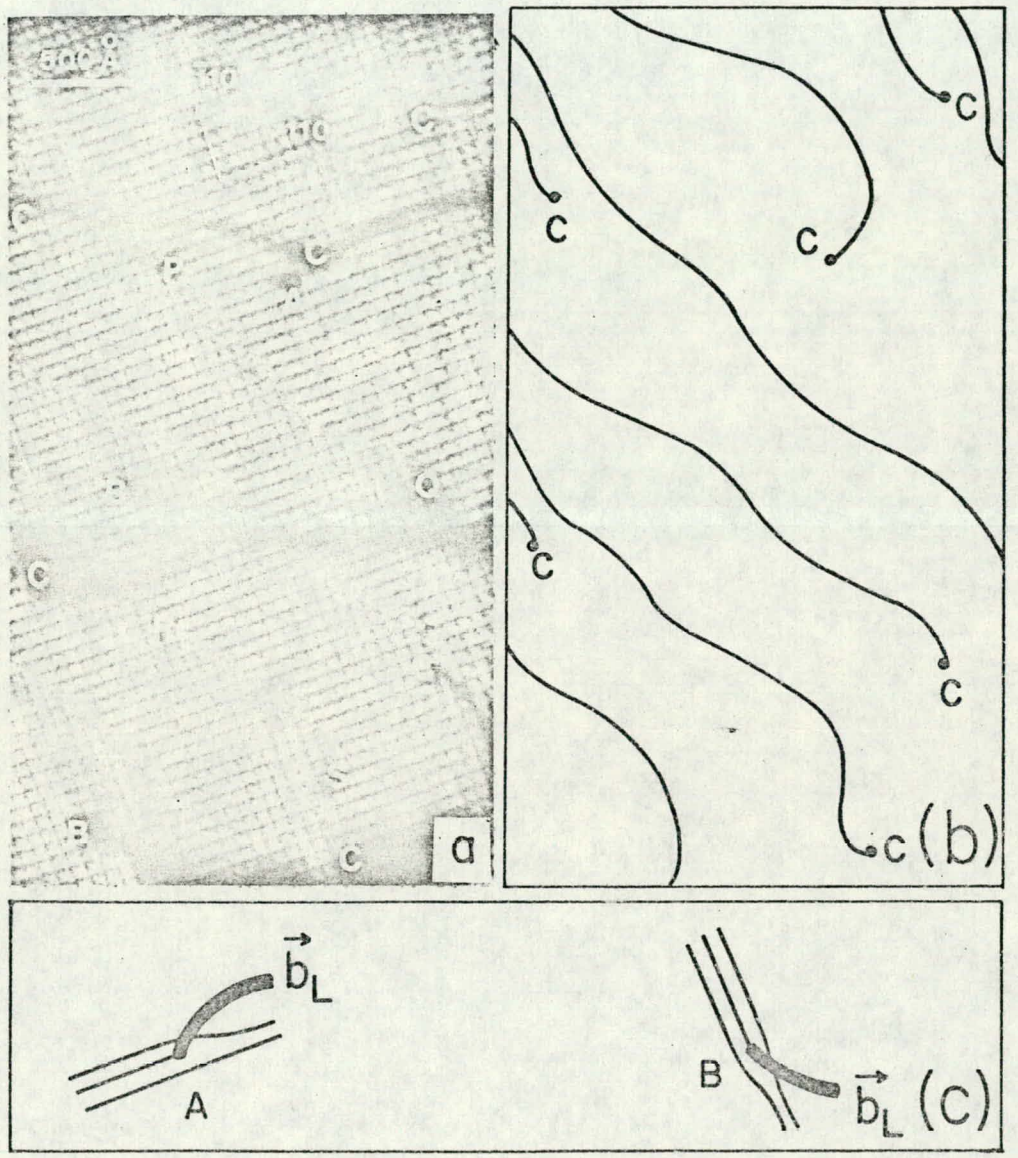

Fig. 1 (Part II)

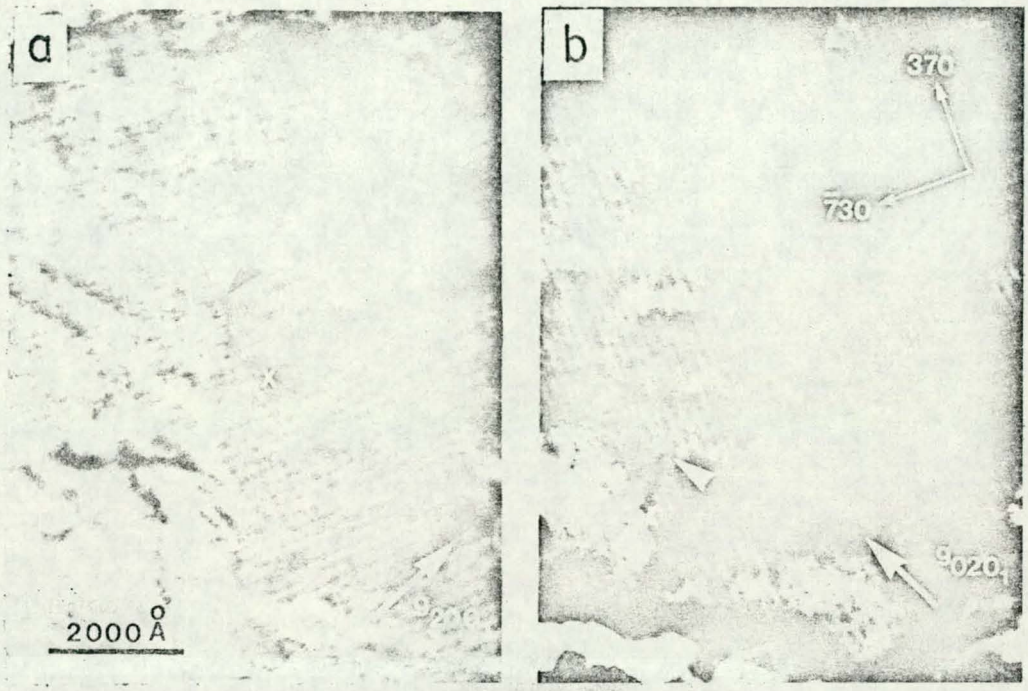
a
2000 Å
b
370
730
0210

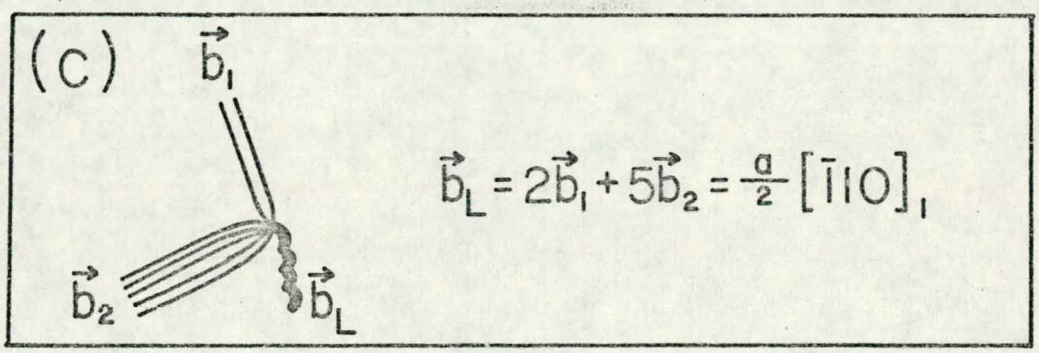
(c)
$\vec{b}_1$
$\vec{b}_2$
$\vec{b}_L$
$\vec{b}_L = 2\vec{b}_1 + 5\vec{b}_2 = \frac{a}{2}[\bar{1}10]_1$

FIG. 2
(Part II)

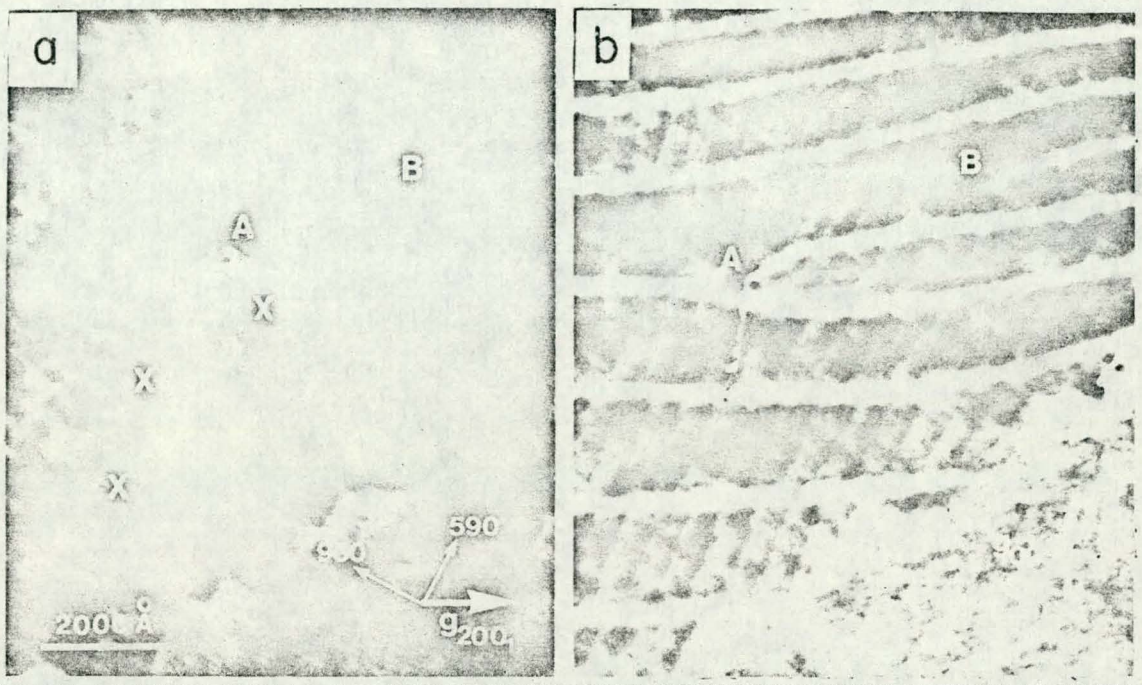

(C)

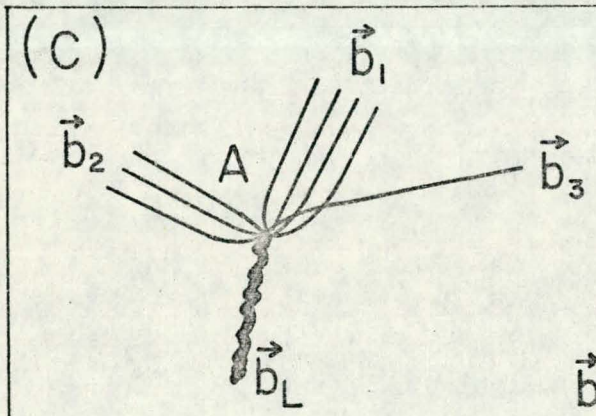

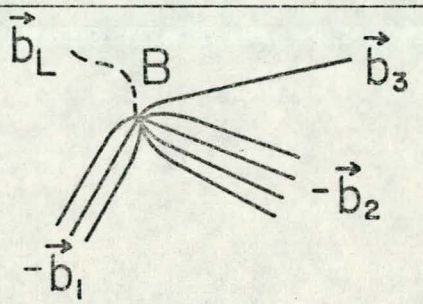

$$\vec{b}_L = -3\vec{b}_1 - 4\vec{b}_2 + \vec{b}_3 = \frac{a}{2}[0\bar{1}1]_2$$

$$\vec{b}_L = 4\vec{b}_1 + 3\vec{b}_2 + \vec{b}_3 = \frac{a}{2}[011]_1$$

FIG. 3 (Part II)

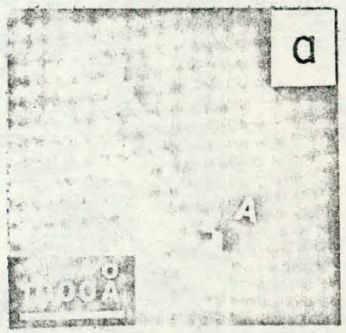

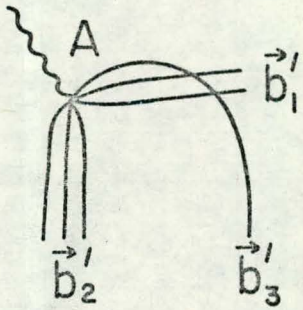

(b)

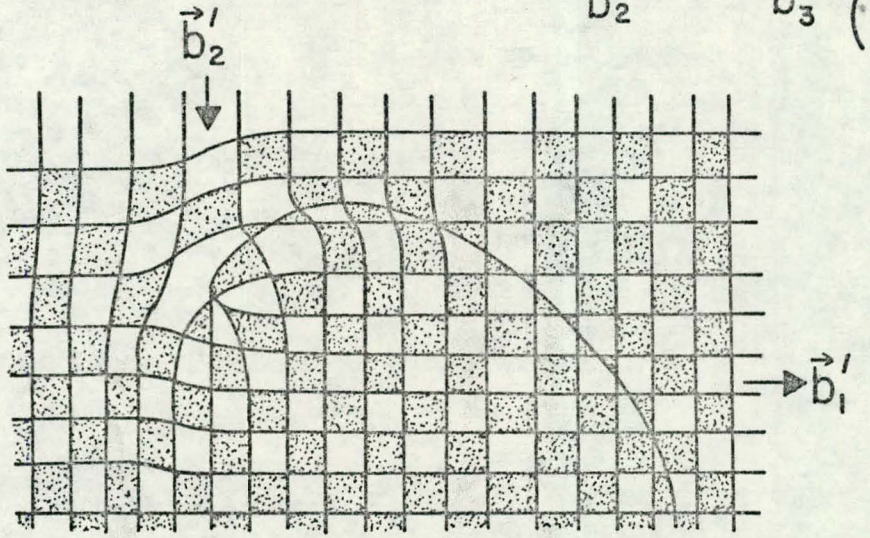

$$\vec{b}_L = 2\vec{b}_1' + 3\vec{b}_2' + \vec{b}_3' = \frac{a}{2}[101]$$

(c)

FIG. 4
(Part II)

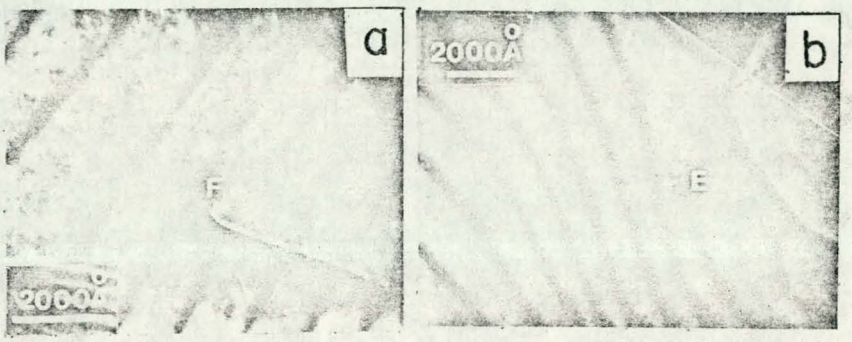

FIG. 5
(Part II)